

Study of the collective activity in neuronal networks through the Izhikevich model: the importance of connectivity

Author: Laia Barjuan i Ballabriga* and Advisor: Dr Jordi Soriano Fradera
Facultat de Física, Universitat de Barcelona, Diagonal 645, 08028 Barcelona, Spain.

Abstract: The Izhikevich description of neuronal behavior is one of the most attractive and successful models in neuroscience since perfectly balances biological plausibility and computational efficiency. Its success has fostered its use to investigate large scale neuronal ensembles and their collective behavior. In the present project two networks of 1000 Izhikevich neurons were setup. The relationship between networks' structural traits and functional organization, which is often characterized by all neurons firing together (*synchronization*), were investigated. The impact of small changes in the parameters of the Izhikevich model and in the connectivity among neurons was also inspected for a better understanding of the behavior of real biological systems upon physical damage or drug action. The results show the potential of the Izhikevich model to draw interesting conclusions on the dynamics of neuronal networks.

I. INTRODUCTION

In recent years, the advancement in the knowledge about the physics of complex systems has fostered a growth of *network neuroscience*, which aims at the characterization and understanding of the mechanisms underlying complex brain structure and function [1]. Networks are mathematical graphs described by nodes and connections that link them. In the context of neuroscience, neurons are the nodes of the networks, whereas synaptic connections or information flow are the connections. To be more precise, two possible representations for a neuronal network are considered, namely *structural connectivity* and *functional connectivity*.

Structural connectivity refers to the physical wiring among neurons, i.e., synaptic connections, while functional connectivity refers to statistical correlations between neurons' activity patterns. For instance, two neurons that activate together frequently would share a strong functional bond, but they are not necessarily physically connected to one another. Since the functional connectivity reflects the communication between neurons across the network, it must be somehow related to the elementary structural links [2]. However, this is not so simple, as we elaborate later. Indeed, one of the most interesting research topics of network neuroscience is the comprehension of the relationship between the structural configuration of a given neuronal network and its functional connectivity.

There is a wealth of evidence indicating that the interplay between topology, neuronal non-linear dynamics and noise (intrinsic to a biological system), shapes the emergence of synchronized collective dynamics characterized by quasi-periodic episodes of high activity also known as *network bursts* [2–4]. However, due to the non-linearity of neuronal circuits a direct relationship between structure and dynamics cannot be established [5].

Consequently, the access to structural information from the analysis of the dynamics of the system is a practically unsolvable inverse problem [6]. Interestingly, this ‘unsolvability’ is what makes neuronals circuits and the brain so powerful: the same structural connectivity can accommodate a rich repertoire of dynamical states or functionalities. To advance in this quest, one of the main goals of the present work is analyzing up to which extent the inferred functional connectivity captures vital features of the network's structural layout. The comparison between structural and functional connectivity maps has been performed using state of the art toolboxes from graph theory [7, 8].

Furthermore, a deep understanding on how brain activity is linked to the structural wiring of the network is pivotal to comprehend its anomalies or malfunctioning due to neurological diseases such as Parkinson's or Alzheimer's [7, 9]. Investigating how networks behave under damage can help us to pave the way towards the treatment of these neuropsychiatric disorders [10]. To gain a deeper insight into this aspect, in this project the damage experienced by the networks due to these diseases was mimicked by gradually removing some of its nodes. In particular, the approach selected for this purpose was the targeted attack on the nodes with highest topological importance (*centrality*).

We note that, typically, when studying neuronal networks, the spatial constraints of the networks are often not taken into account, i.e, neurons and connections are laid on a topological mathematical space without metrics, so that the actual distance between neurons is irrelevant. In reality, the brain is organized into physical columns and layers, while neuronal cultures (neurons grown on glass) are embedded on a rigid bi-dimensional substrate. In this sense, it is known that brain areas that are close in space have higher probability to connect than remote regions [7, 11]. Thus, seeking a more realistic representation, in the present study we built directed networks embedded in a two-dimensional Euclidean space. In addition, the links between neurons have been chosen to be weighted, hence in real cases the capacity and intensity

*Electronic address: lbarjuba8@alumnes.ub.edu

of connections are heterogeneous [8].

Regarding the dynamics of the system, usually what interests neuroscientists is the analysis of the collective activity of the network instead of a detailed physico-mathematical description of the local behavior of neurons. Thus, the dynamics is portrayed by a simple yet powerful biologically-inspired model. In particular, in this project a slightly modified version of the original Izhikevich model [12] was employed. This Izhikevich model is a smart simplification of the FitzHugh–Nagumo model, a vastly used model for neurons, and that in turn is a simplification of the Hodgkin–Huxley model, the almost-perfect description of a neuron (Nobel Prize in 1963) but that requires super-computers to operate with it.

II. NETWORK GENERATION

The numerical simulations carried out considered weighted directed spatial *in silico* networks of $N = 1000$ neurons set on a two-dimensional circular area of 8.4 mm in diameter. Since real neurons are not laid out on a grid, but are rather distributed in space with some heterogeneity [6], we generated aggregated networks (Fig. 1) where the N neurons were divided into various subsets of equal number of neurons. In particular, in the two networks analyzed, neurons were split into five and ten islands respectively, randomly distributed over the surface. The construction of the networks took the following steps:

1. First of all, the coordinates of the subsets' centers were randomly selected using polar coordinates. They were located at most at $r = 3$ mm from the origin of coordinates.
2. Then, the neurons corresponding to each island were placed arbitrarily with its coordinates following a Gaussian distribution centered at each island center.
3. A connection between neurons i and j was established whenever the distance between them was smaller than a threshold d_{\max} , so that nearby neurons were more connected. Initially all connections were set as excitatory with its weights, w_{ij} , following a Gaussian distribution with $\mu = 0.6$ and $\sigma = 0.06$. Table I summarizes the parameters used. The whole network connectivity was stored in the structural matrix $\mathbf{W} = \{w_{ij}\}$, where the rows corresponded to the outgoing connections $i \rightarrow j$ and the columns to the ingoing ones $i \leftarrow j$. Considering that the simulated networks were directed, the structural matrix was not symmetric: $w_{i \rightarrow j} \neq w_{j \rightarrow i}$.
4. Afterwards, 20% of the neurons were selected randomly and converted to inhibitory neurons according to the Dale's principle [13], which postulates

that all outgoing connections of a neuron are either excitatory or inhibitory, i.e., an excitatory neuron for instance only projects excitatory connections. Therefore, the transformation of the selected neurons was performed by switching all their outgoing connections to inhibitory: their weights were multiplied by a factor $-1/6$.

5. Finally, pursuing a more realistic layout of connectivity, 90% of the original connections were randomly removed, so that neurons on average had about 100 neurons. To many connections shape networks in which a neuron almost connects with any other, which is neither realistic nor interesting.

Network parameters		
	Excitatory	Inhibitory
Number of neurons	$N = 1000$	
Surface diameter	$\phi = 8.4$ mm	
σ of island diameter	$\sigma_\phi = 0.3$ mm	
Maximum connection distance	$d_{\max} = 1.41$ mm	
% of connections allowed	10%	
% of inhibition	20%	
Mean connection weight	$\mu = 0.6$	$\mu = -0.1$
σ connection weight	$\sigma_w = 0.06$	$\sigma_w = 0.01$

TABLE I: Structural parameters of the *in silico* networks.

Due to the metric construction of the network distinct connectivity arrangements can be obtained from realization to realization. Representative graphs of two networks under study and their structural connectivity matrices are presented in Fig. 1.

III. DYNAMICAL MODEL

A neuron can be described as an electrically excitable cell which reacts to inputs from other neurons generating electrical impulses that propagate as action potentials. The membrane potential v is the key variable for the description of a firing neuron and it can be defined as the difference in the electric potential between the interior and the exterior of the cell caused by the gradient of concentration of ions. When a neuron receives a stimulus, its membrane potential increases (decreases) if the input is excitatory (inhibitory). A typical value of the resting potential, i.e., in the absence of any stimulus, is -60 mV. The aforementioned action potentials are sudden, fast, transitory, and propagating changes of the resting membrane potential, i.e., they are what neuroscientists call *spikes*. Spikes are generated when the negative inside potential reaches a threshold and increases abruptly (*firing* of the neuron). Action potentials are propagated through the neuron's axon and are vital for the communication among neurons through synapses. The complex processing of neuronal inputs and outputs confers a neuron its 'integrate-and-fire' non-linear behavior [14–16].

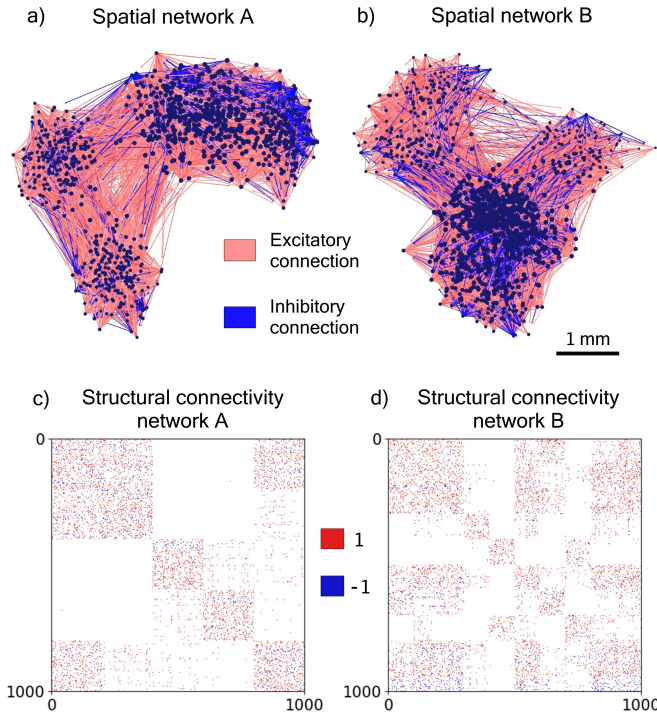


FIG. 1: (Top) Directed graphs of two simulated networks. Excitatory connections represented in red and inhibitory connections in blue. Darker colors are related to stronger connections. Each black dot corresponds to a neuron. The size of the dots is directly proportional to the number of connections of the neuron it represents. (Bottom) Structural matrices of the two networks where all excitatory connections have been set to 1 and all inhibitory to -1 . Each matrix corresponds to the graph immediately above.

In 1952 Hodgkin and Huxley [17] described the flow of electric current through the membrane with a model consisting of four equations and tens of parameters. This model, although being very accurate from a biological point of view, is extremely complex and impractical for the study of large neuronal systems. On the other hand, the most popular and computationally–biophysically friendly model of neuronal dynamics is the generally called ‘integrate-and–fire’, which uses a single equation with four parameters and can reproduce quite well the behavior of neurons. The FitzHugh–Nagumo and the Izhikevich models are the most famous ones of this type.

In this project we have used the Izhikevich model for spiking neurons [12]. This model is a super–simplification of the Hodgkin–Huxley model, but maintains its biological plausibility while being as computationally feasible as an integrate–and–fire model. The Izhikevich model can reproduce rich firing patterns, such as spiking and bursting, of different types of real cortical neurons and, at the same time, its computational simplicity enables it to simulate thousands of neurons in real time in a personal computer.

The model is based on the resolution of a system of

two ordinary differential equations:

$$\frac{dv}{dt} = 0.04v^2 + 5v + 140 - u + I, \quad (1)$$

$$\frac{du}{dt} = a(bv - u), \quad (2)$$

with the after-spike resetting

$$\text{if } v \geq 30 \text{ mV, then } \begin{cases} v & \leftarrow c \\ u & \leftarrow u + d. \end{cases} \quad (3)$$

where v represents the membrane potential of the neuron, u a recovery potential that helps returning the system to the resting state and I the synaptic current received by the neuron. The parameter a describes the time scale of u ; b is related to the sensitivity of u to subthreshold fluctuations of v ; c is the after-spike reset value of v ; and d is the after-spike reset value of u . Their specific values depend on the type of cortical neuron simulated and are chosen randomly from a range of values, see Table II, at the beginning of the simulation.

The synaptic current has been modeled following the approach of Hernández–Navarro *et al.* [18]. Considering that the emission of a pulse from neuron i at time t_p induces a postsynaptic current in neuron j , the total synaptic current received by the neuron j can be computed as

$$I_j(t) = \eta + \sum_{i=1}^N \sum_{t_p < t} w_{ij} E_i(t, t_p), \quad (4)$$

$$E_i(t, t_p) = g_A D_i \exp\left(-\frac{t - t_p}{\tau_A}\right) \Theta(t - t_p), \quad (5)$$

$$\frac{dD_i}{dt} = \frac{1 - D_i}{\tau_D} - (1 - \beta) D_i \delta(t - t_p), \quad (6)$$

where η is a noisy input, w_{ij} is the connection weight between neurons i and j and $E_i(t, t_p)$ is the current induced by the neuron i at time t as a result of a spike generated at time t_p . g_A is the strength of the synapse and τ_A represents its decay time. D_i is the depression term and is related to the reduction of efficiency of synaptic connections after a spike. At the beginning of the simulation this term is set to 1. β represents the loss of efficiency of the synaptic connection when the neuron fires and τ_D is the characteristic depression decay time.

All the parameters used in the simulation are indicated in Table II.

The evolution of the membrane potential of an excitatory neuron and ‘raster plot’ obtained after the simulation of the dynamics of network A (Fig. 1a) is presented in Fig. 2. A raster plot shows the activity of a neuron at a given time as dot on a neurons–time graph. The raster plot shows that many neurons activated quasi-synchronously within a narrow time window. This reflects the existence of collective, coordinated activity, and that normally coexists with sporadic individual activations of the neurons. A similar figure could be obtained for the network B of Fig. 1b.

Model parameters		
	Excitatory	Inhibitory
Time scale of u	$a = 0.02$	$a = [0.02, 0.1]$
Sensitivity of u	$b = 0.2$	$b = [0.2, 0.25]$
Resting potential (v)	$c = [-65, -50] \text{ mV}$	$c = -65 \text{ mV}$
Reset value of u	$d = [2, 8] \text{ mV}$	$d = 2 \text{ mV}$
Threshold potential	$v = 30 \text{ mV}$	$v = 30 \text{ mV}$
Initial potential	$v = -65 \text{ mV}$	$v = -65 \text{ mV}$
Algorithm	Euler	
Integration time	3 s	
Time step	$\Delta t = 1 \text{ ms}$	
Synapse parameters		
Noise	$\eta = [0, 5] \text{ mV}$	
Synapse strength	$g_A = 3 \text{ mV}$	
Synapse decay time	$\tau_A = 5 \text{ ms}$	
Depression recovery time	$\tau_D = 1000 \text{ ms}$	
Depression decay	$\beta = 0.6$	

TABLE II: Dynamical parameters of the simulation.

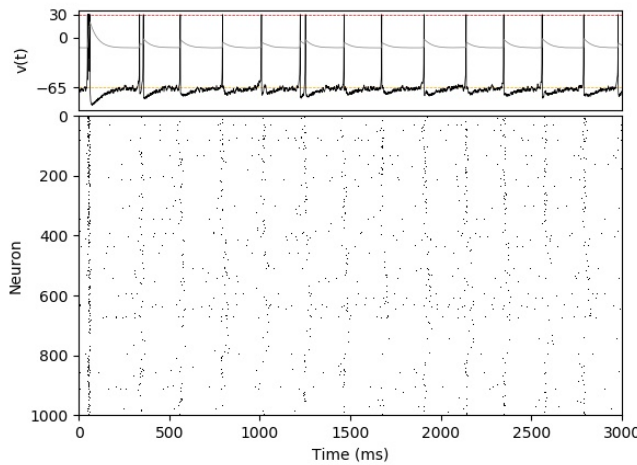


FIG. 2: (Top) Representative time evolution of the membrane potential v of an excitatory neuron. The orange dashed line at $v \approx -65 \text{ mV}$ corresponds to the resting initial potential, the red dashed line at $v \approx 30 \text{ mV}$ to the threshold potential and the grey curve to the evolution of the recovery potential. (Bottom) Raster plot of the network. Collective neuronal activations appear as vertical bands of synchronous activity, with a frequency of 4.5 Hz, that is combined with single neuron firings.

IV. NETWORK ANALYSIS

The graph theory offers a set of measures and tools to quantitatively characterize networks. In this framework, biological neuronal networks can be described as graphs composed of nodes denoting neurons that are linked by edges representing physical or functional connections between them [7]. Therefore, in the past years the mathematical treatment of complex networks provided by graph theory has been widely used in network neuroscience. In this section we introduce the definitions of the quantities used to describe the topology of the

simulated networks [1, 8]. These magnitudes have been computed using the Brain Connectivity Toolbox and Networkx of python.

A. Node degree

The degree of a node is the number of connections that links it to the rest of the network [7]. In directed graphs it is computed as $k_i = k_i^{\text{out}} + k_i^{\text{in}}$ where k_i^{out} are the outgoing connections from neuron i and k_i^{in} the ingoing ones.

The degree distribution is the probability distribution of all node degrees and is a fundamental property of the network.

B. Modularity

The modularity, Q , quantifies the likelihood that neurons group into communities (modules). It measures the correlation between the probability of having a connection between two neurons and the fact that they belong to the same module [8]. In other words, a community exists when the neurons within the community are more connected with themselves than with the rest of the network.

Having a $Q \rightarrow 1$ indicates that the network is strongly modular, i.e., its neurons tend to have more intra- than intermodular connections. However, $Q \simeq 0$ suggests that the neurons constituting the network are connected indiscriminately, and therefore the network itself is the only community.

The Brain Connectivity toolbox uses the Louvain algorithm to compute this magnitude [19].

C. Global and Local Efficiency

The **Global Efficiency** E_{glob} indicates the integration capacity of the network. In other words, it is a measure of the efficiency of information exchange among neurons across the network. It can be defined as the average of the inverse shortest path lengths, which are the minimum topological distances between two neurons:

$$E_{\text{glob}} = \frac{1}{N(N-1)} \sum_{j \neq i} \frac{1}{d_{ij}}, \quad (7)$$

where N is the total number of neurons and d_{ij} denotes the shortest weighted path length between neurons i and j [8]. Disconnected nodes have $d_{ij} = \infty$ and do not contribute to the sum. Since shorter connection lengths are associated with higher connection weights, the global efficiency is also related to the connection weights between neurons.

Eq. (7) discloses that high global efficiencies ($E_{\text{glob}} \simeq 1$) correspond to networks with a strong degree of integration i.e., with short topological distances

between neurons, whereas modular networks have lower values of this magnitude ($E_{\text{glob}} \simeq 0$).

The **Local Efficiency** E_{loc} is the average of the efficiencies computed at the neighborhood of each node. It is given by

$$E_{\text{loc}} = \frac{1}{N} \sum_i E(G_i), \quad (8)$$

where $E(G_i)$ is calculated as in Eq. (7) but in the local subgraph G_i that consists of the immediate neighbors of node i but not i itself. A high value of this magnitude suggests a modular network whereas a low value corresponds to an integrated network.

D. Betweenness centrality and robustness

The **betweenness centrality (BC)** of a node is a measure of its relevance to the efficient communication of the network. It can be measured counting how many of the shortest path lengths between all other node pairs pass through it.

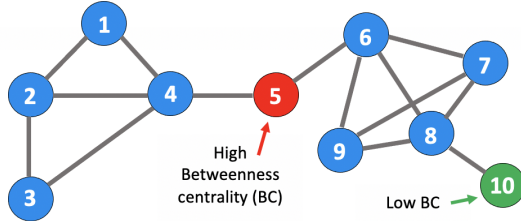


FIG. 3: Illustrative graph in which the node with highest BC is highlighted in red (number 5) and the node with lowest BC is in green (number 10).

The **robustness** of a network refers to its ability to maintain its major structural integrity and overall dynamical traits, avoiding malfunctioning when a fraction of its nodes have been deleted.

E. Cross correlation

In this project, the functional correlation between neurons was calculated by means of the pairwise Pearson Correlation Coefficients. The correlation coefficient between neurons i and j was obtained by computing the correlation between their corresponding rows in the raster plot using the expression:

$$r_{ij} = \frac{\sum_t [x_i(t) - \bar{x}_i][x_j(t) - \bar{x}_j]}{\sqrt{\sum_t [x_i(t) - \bar{x}_i]^2} \sqrt{\sum_t [x_j(t) - \bar{x}_j]^2}}, \quad (9)$$

where $x_i(t)$ is the binary signal equal to 1 in presence of a spike at time t and 0 otherwise, and \bar{x}_i is the time averaged value [20]. r_{ij} will tend to 1 whenever the neurons

fire synchronously and to 0 whenever they are dynamically independent (activate randomly). These coefficients r_{ij} are our definition of ‘statistical relationship’ in activity patterns, therefore shape our ‘functional’ network and thus are stored in the functional connectivity matrix, $\mathbf{A} = \{a_{ij}\}$.

1. Surrogates

The aforementioned functional matrix may contain some spurious connections, i.e. correlations among activity patterns that are similar to those occurring just by random activity. Thus, they must be removed in order to obtain reliable functional connectivity data. These spurious correlations are filtered out using a confidence threshold obtained from *surrogates*.

Surrogates are randomized time series of firing events that preserve the total number of spikes per neuron while destroying the intrinsic time correlation between them. In this project, surrogates have been obtained by randomly moving each spike two or three time units forward or backward.

Surrogates are used to create null models of connectivity matrices [6]. The average value of the weights of these matrices plus two times its standard deviation is used as a lower cut-off threshold for the original matrix, i.e., all the original functional weights smaller than this cut-off are set to 0. With the objective of attaining better results, five surrogates were computed for each simulation.

V. RESULTS AND DISCUSSION

A. Impact of connectivity and of Izhikevich’s coefficients

A preliminary study of the original Izhikevich model [12], i.e., without the depression term, was performed. The influence of the model’s parameters and of the degree of integration of the network in the emergence of collective activity was investigated. To achieve these goals we have used a simplified network with two modules of 500 neurons and a maximum distance of connection $d_{\text{max}} = 1.41$ mm. The mean values of the strength of connection, of percentage of inhibition and of noise were set as in the original article [12]: $\mu_{\text{exc}} = 0.5$, $\mu_{\text{inh}} = -1.0$, 20%, $\eta_{\text{exc}} = [0, 5]$ mV and $\eta_{\text{inh}} = [0, 2]$ mV.

First of all, we wanted to study the impact of the degree of integration of the network on the appearance of collective dynamics (*bursts*). Initially all possible connections due to metric restrictions were regarded and they were progressively removed until the collective activity ceased. The critical value of connectivity was found when half of the connections were deleted. At this point, sometimes the network exhibited bursts and sometimes neurons fired asynchronously.

We can see in Fig. 4 that the intensity of network bursts decreases as a result of the reduction in the number of

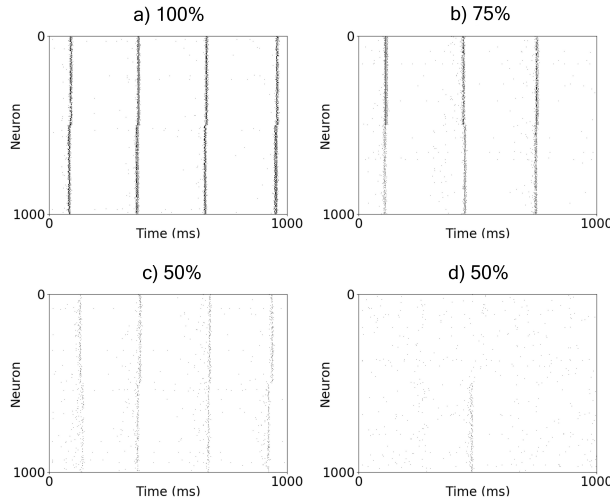


FIG. 4: Network bursts of a two-module network for different values of percentage of allowed connections among neurons.

connections between neurons. When the 50% of connections were removed, two possible scenarios emerged: in Fig. 4c the system shows weak synchronous collective activity whereas in Fig. 4d there is only a single one-module burst at approximately $t = 500$ ms. For lower values of connectivity not even single-module bursts were observed. In conclusion, we have found that a strong connectivity and intercommunication among neurons favors the formation of network-spanning activations, a network property also highlighted by Faci-Lázaro *et al.* [10].

Another important aspect to be considered regarding the appearance of collective activity is the intensity of connections. In order to study this effect we have chosen the previous network with 10% of connections and we varied the weights of the synapses between neurons. With the original Izhikevich's weight parameters neurons fired asynchronously. However, as we increased the weight of excitatory connections and decreased the one of inhibitory links, in absolute value, network bursts reappeared. For $\mu_{\text{exc}} = 2$ mV and $\mu_{\text{inh}} = -0.4$ mV we obtained collective neuronal activations almost identical to the ones for the previous values of μ and with 100% of connections. Therefore, a decrease in the degree of network integration can be compensated by an increase in the intensity of connections between neurons.

So far we only studied the transition from erratic activity to full coherence due to the connectivity traits of the network. We now analyse the effect of the variation of the phenomenological parameters of the model. We performed the simulations with the matrix we have just found ($\mu_{\text{exc}} = 2$ mV and $\mu_{\text{inh}} = -0.4$ mV) but with noise values set to $\eta = [0, 5]$ mV for both inhibitory and excitatory neurons.

Several studies investigated the emergence of bursts with different oscillation frequencies in a network of Izhikevich neurons by tuning the parameters of the model [21, 22]. These studies mainly pinpointed the

role of the variation of parameters a and b and observed that the Izhikevich model was capable of showing network bursts with frequencies ranging from 4 to 40 Hz. In the present work, we examined how changing the fixed coefficients of Eq. (1) influences the frequency of collective activations. The study was performed changing only one parameter at a time and the results obtained are displayed in Table III.

$\alpha \cdot v^2$	Hz	$\gamma \cdot v$	Hz	140	Hz
$\alpha \leq 0.03$	No bursts	$\gamma = 4.5$	26	≤ 139	No bursts
$\alpha = 0.04$	4	$\gamma = 4.9$	11	140	4
$\alpha = 0.05$	26	$\gamma = 5$	4	150	13
		$\gamma = 5.1$	No bursts	170	22

TABLE III: Frequencies of network bursts obtained after varying the coefficients in Eq. (1).

In the table we can see that a small variation in these parameters triggers a drastic change to the rhythm of networks bursts, which never occur at frequencies lower than 4 Hz. These results are in accordance with the ones in the bibliography.

B. Comparison between structural and functional networks

Up to now, the results analyzed were obtained using the parameters exposed in Sections II and III. These parameters were selected after several tests because they were the ones that provided more realistic results.

The resemblance between the structural and functional matrices was evaluated through the computation of the magnitudes from graph theory (network measures) explained in Section II. We first calculated these quantities for the structural connectivity and afterwards for the functional one of the two networks studied.

To shed light on the importance of spatial embedding all magnitudes were also computed for two null models: a randomly rewired network and an equivalent Erdős-Rényi (ER) random network. A rewired network is obtained by randomly reassigning the outgoing connections of every neuron. As a result, metric correlations are erased but the total number of outgoing connections of each neuron is conserved. The Erdős-Rényi random graphs are uncorrelated graphs where a link between two neurons has a fixed probability of being present or absent, independently of the others. Consequently, all nodes in ER graphs are statistically equivalent and for a large number of nodes their degree distribution approach a Poisson distribution [8, 23]. ER graphs were computed using a probability of connection that reflects the node degree of the desired network.

• Structural analysis

The structural networks analyzed are the ones presented in Fig. 1. These networks have been designed in

such a way that spatial constraints influence their connectivity, i.e., neurons have a greater probability of being connected to nearby neurons than to far away ones. Therefore, we expect neurons to be fairly aggregated, with well-defined modules. The distributions of node degrees of both networks are depicted in Fig. 5.

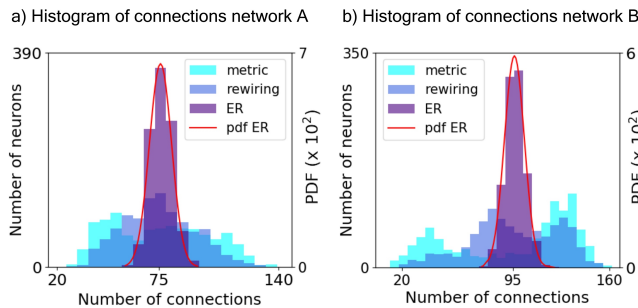


FIG. 5: Histogram of connections of the metric (cyan), random rewired (blue) and ER random (purple) structural networks. The Poissonian distribution function corresponding to the ER network is displayed in red. Binwidths=6.

This figure shows that the histogram of connections of the metric matrices are broader and therefore flatter than the ones of the ER random networks. In the metric networks, neurons with a very small number of connections, about 20, coexist with neurons with a really high node degree, 140 in network A and 160 in network B. This variety is due to the position of the neuron within the network, i.e., whether its location allows it to have many connections or not. It can also be seen that the distribution of connections of the ER random graph follows a Poissonian distribution, as expected. In its turn, the rewired network shows a tendency to have a Gaussian shape. In fact, if there were infinite nodes the two null models should practically coincide.

A more exhaustive analysis of the networks can be performed by computing their average node degree, modularity, global and local efficiencies. These results are presented in Table IV.

In that table one can see that network A has a smaller average node degree than network B, which translates to a greater modularity. In fact, modules appear well-defined if $Q > 0.2$ and the value of modularity of network B is close to this value. On the other hand, the local efficiency of both networks is bigger than the global efficiency. This indicates that these networks are more efficient exchanging information at a local scale than at a global scale, which is a characteristic trait of aggregated networks.

As expected, both rewired networks have small values of modularity and their global efficiency is bigger or almost equal to the local. This is due to the fact that after the random rewiring some neurons that originally could not connect because of metric restrictions have now a link between them. However, these long-distance connections have been established at the expense of short-range one.

	Network A	Network B
Average node degree	74.87	95.09
Metric		
Number of modules	4	5
Modularity (Q)	0.41	0.23
Global Efficiency	0.26	0.29
Local Efficiency	0.39	0.39
Rewired		
Number of modules	Not defined	Not defined
Modularity (Q)	0.18	0.12
Global Efficiency	0.29	0.30
Local Efficiency	0.19	0.31
ER		
Number of modules	Not defined	Not defined
Modularity (Q)	0.10	0.10
Global Efficiency	0.29	0.32
Local Efficiency	0.30	0.38

TABLE IV: Network measures of structural connectivity for networks A and B and their corresponding null models.

Consequently, the previous modules have been blurred while favouring a more efficient exchange of information at a global scale.

Finally, the ER random network has a value of modularity very close to 0, which is associated to a fully integrated network with one module. With regard to the global and local efficiencies it can be observed that, contrary to what we would expect for a completely randomly constructed network, the global efficiency is slightly smaller than the local. However, this is due to the randomness of the network and if we performed several realizations and computed the mean value of these two quantities they would end up having similar values.

Another noteworthy fact is that, as expected, the value of global efficiency of both networks grows as the randomness in the construction of the network increases.

• Functional analysis

The functional connectivities were inferred from the analysis of the raster plots using cross correlation, as described in Section IV. This type of statistical correlation has the same value regardless of the direction of the connection, see Eq. (9). Therefore, functional graphs are undirected and their functional connectivity matrices are symmetric. The resulting functional networks and their connectivity matrices are displayed in Fig. 6.

It is interesting to note from Fig. 6 that in both networks the neurons with more connections (represented by bigger dots) are concentrated in the larger module. In contrast, the neurons that make up small modules exchange less information with the rest of the network.

Even though the structural graphs of both networks (Fig. 1) seem pretty alike, with a distinguishable large module and two smaller ones, all of them interlinked, the analysis of their functional connectivities, portrayed in Fig. 6, unveils that the neurons conforming the two small aggregates of network B are much less connected to the rest of the network than the ones of network A.

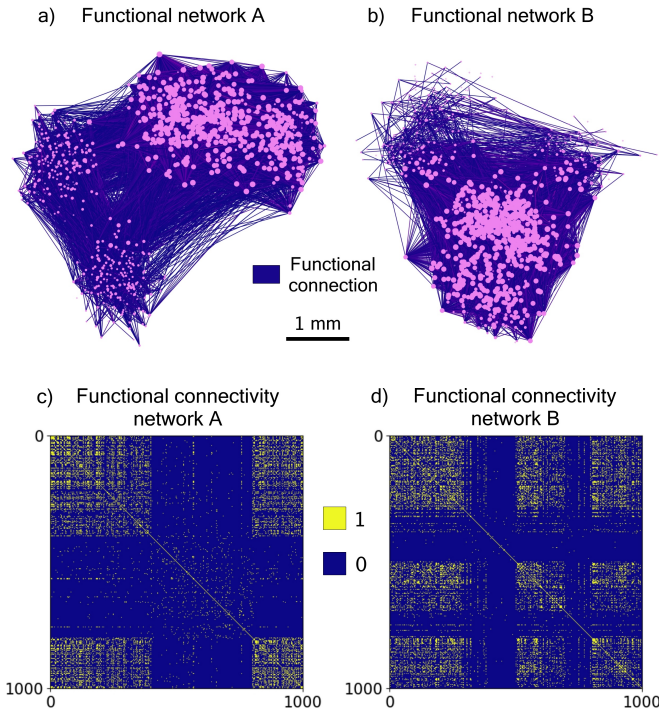


FIG. 6: Functional analysis of representative networks. (Top) Undirected graphs of the two functional networks. All functional connections are represented in purple. Brighter tones are related to stronger connections. Each pink dot corresponds to a neuron. The size of the dot is directly proportional to the number of connections of the neuron it represents. (Bottom) Functional matrices of the two networks where all connections with a weight bigger than the cutoff obtained from surrogates have been set to 1 and all the others to 0. The cutoff value for network A is $w_c = 0.18$ and for network B is $w_c = 0.21$. Each matrix corresponds to the graph immediately above.

The histogram of functional connections of both networks is displayed in Fig. 7. In this figure one can see that the distributions of connections of the functional networks cover a very wide range of values. One noteworthy fact is that several neurons have really small values of connectivity: approximately 300 neurons in each network are linked to less than fifteen other neurons. On the contrary, some neurons are very connected to the rest of the system, with about 250 links in network A and 300 in network B.

Regarding the network properties calculated by means of the graph theory, for the functional cases only the metric and rewired matrices have been studied. Their values of the average node degree, modularity, global and local efficiencies are presented in Table V.

In Table V one can see that both networks have a high value of modularity. Therefore, their global efficiency is almost zero and both networks are really inefficient at exchanging information across them. Their communication at a local scale is notoriously better but not very efficient either. As observed in the structural analysis,

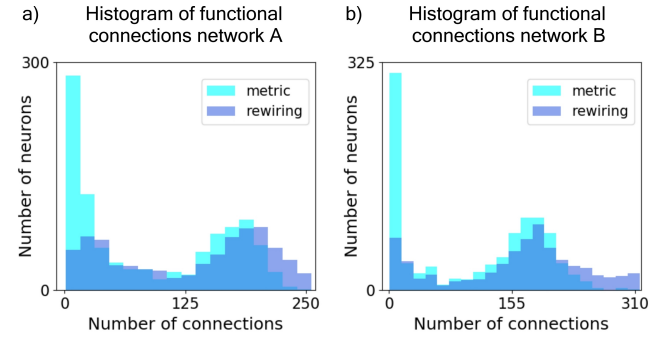


FIG. 7: Histogram of functional connections of the metric (cyan) and random rewired (blue) functional networks. Bin-widths=15.

	Network A	Network B
Average node degree	88.24	107.11
Metric		
Number of modules	9	8
Modularity (\mathcal{Q})	0.49	0.41
Global Efficiency	0.10	0.11
Local Efficiency	0.20	0.22
Rewired		
Number of modules	2	4
Modularity (\mathcal{Q})	0.27	0.22
Global Efficiency	0.15	0.17
Local Efficiency	0.12	0.15

TABLE V: Graph theory magnitudes of the functional connectivity matrices of networks A and B and their corresponding rewired networks.

the modularity of the rewired networks is smaller than the one of the metric networks. Furthermore, the global and local efficiencies follow the same behavioral pattern as before: the global efficiency increases at the expense of a decrease in the local efficiency.

• Comparison of structure and function

A first rough evaluation of the similitude of the structural and functional networks can be done by comparing the magnitudes gathered in Tables IV (structural) and V (functional). Comparison of course only makes sense for the metric networks. It is interesting to notice that both functional networks have a higher average node degree than the corresponding structural networks. Moreover, the number of modules of the functional networks is approximately double that of the structural networks. Considering that their modularities are also higher, we can hypothesize that the actual exchange of information across the network happens to concentrate preferably between neighboring neurons than between distant neurons, i.e., the network does not take advantage of all potential pathways provided by the structural wiring. A plausible explanation is that neurons that are located very close together are creating functional nuclei since the communication between them is easier. This behavior was also observed by Tibau et al. [6]. In addition, the global and

local efficiencies, although showing a very similar relative behavior, have very different numerical values.

Another interesting approach to visually portray the difference between the structural and functional links is the representation of the 5 % most important connections of each network. These graphs are depicted in Fig. 8.

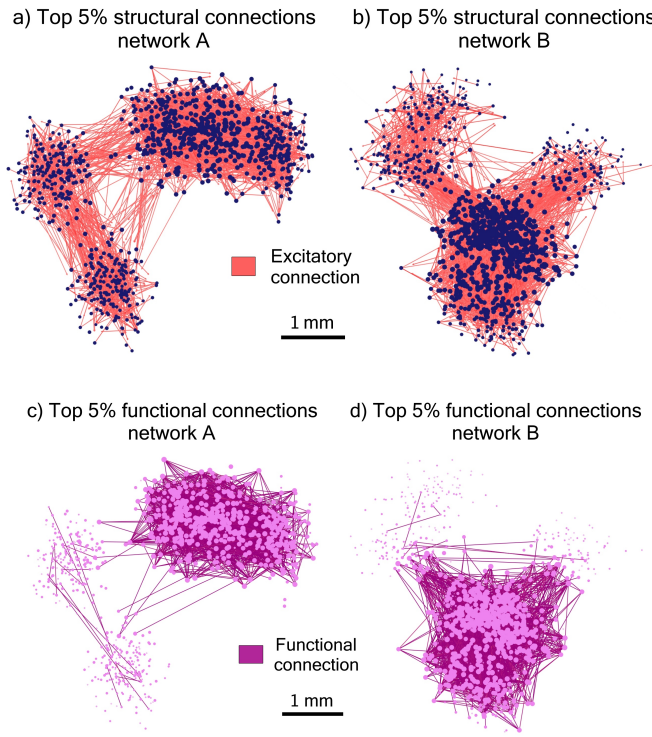


FIG. 8: Comparison of structural and functional networks. (Top) Directed graphs of the two structural networks where only the top 5% stronger connections are represented in red (excitatory). Darker tones are related to stronger connections. Each black dot corresponds to a neuron. (Bottom) Undirected graphs of the two functional networks where only the top 5% stronger connections are represented in violet. Brighter tones are related to stronger connections. Each pink dot corresponds to a neuron. In all graphs the size of the dots is directly proportional to the number of connections of the neuron it represents.

The analysis of Fig. 8 discloses that whereas the stronger physical connections are approximately homogeneously distributed all over the network, the most important functional links are almost entirely gathered inside the largest module. Thus, it can be stated that the strongest physical connections are not necessarily relevant from the point of view of system dynamics.

Another particularly interesting magnitude which can help us reflect the difference between the structural and functional networks is the percentage of structural links that actually act as functional pathways. For network A the percentage obtained is 9.06% and for network B it is 8.75%. That is, about 10% of the structural connections happen to serve as a functional link between neurons.

• Node importance: Betweenness centrality

The study of the nodes' betweenness centrality (BC) can also be enlightening in the distinction between structural and functional networks. The results obtained after the calculation of this magnitude for our networks are displayed in Fig. 9.

In this figure one can see that even though both spatial networks seem pretty alike at first glance, the curves of their values of BC displayed in Figs. 9a and 9b are very different. The structural network A has very few nodes with huge values of BC, and decays so fast that its the curve of BC resembles a scale-free behavior, i.e. with very few highly important nodes whose loss can be dangerous. On the other hand, network B has a flatter structural BC curve. This means that the potential communication pathways are distributed more equally among all the nodes, i.e., there is not one crucial node for a proper integration of the network. This last statement is also reinforced by the comparison of the maximum value of BC of each network: it is more than three times bigger in network A than in network B. Thus, less shortest paths between nodes of the network pass through the most central node of network B. Concerning the functional curves, both of them have very similar shapes and their maximum values do not diverge excessively. In light of these results we can conjecture that the extraction of the structural network from the functional one is a complicated task since similar functional connectivities can emerge from very different structural layouts.

In addition, in Figs. 9c and 9e for network A, and Figs. 9d and 9f for network B, one can quickly see that the nodes with the highest value of BC are different in the structural and functional networks. Whereas the most central nodes in the structural networks are located in the region of connection between modules, the nodes with highest BC of the functional network is placed in the middle of the largest module. In fact, if we compare the top 5% of nodes with highest betweenness centrality of the structural and functional networks, only the 14% match for network A and the 4% for network B.

C. Targetted attack

As mentioned in the introduction of the project, the analysis of the relationship between the structure of a network and its dynamics is incredibly useful to tackle neurodegenerative diseases. These disorders are associated with altered synchronization patterns caused by a deterioration of the organization of neuronal circuits due to a significant loss of highly central neurons [24, 25]. The failure of this type of neurons compromises the functionality of the system because they act as routes of information flow across the network [2].

To assess the resilience of the neuronal circuits to damage caused by the loss of neurons we explored the capacity of our networks to preserve their collective activity

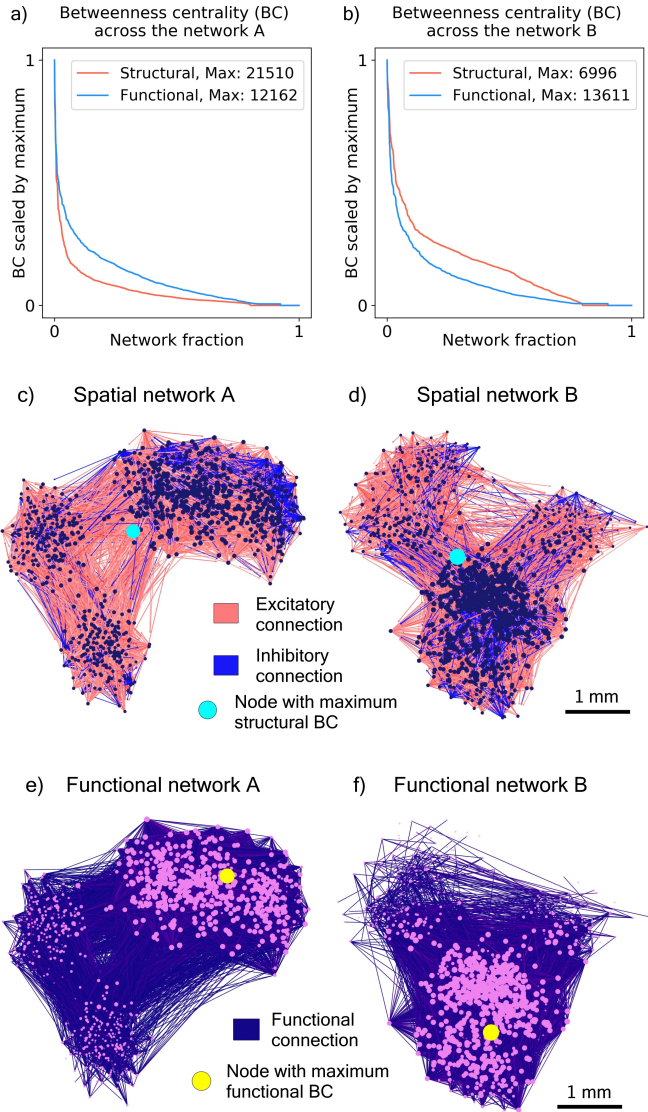


FIG. 9: Node importance and centrality in structural and functional networks. (Top) Betweenness centrality of all neurons arranged in descending order. The maximum value of BC of each network is indicated in the legend. (Middle) Directed graphs of the structural networks. Excitatory connections are represented in red and inhibitory connections in blue. Darker tones are related to stronger connections. Each black dot corresponds to a neuron and the cyan dot is the node with highest BC. (Bottom) Undirected graphs of the functional networks. Connections are represented in violet and brighter tones are related to stronger connections. Each pink dot corresponds to a neuron and the yellow dot is the node with highest BC. In all graphs the size of each dot is directly proportional to the number of connections of the neuron it represents. The size of the nodes with maximum BC has been augmented for the seek of an easier identification.

upon damage. In particular, we focused on the deletion of nodes with highest structural betweenness centrality and we evaluated the structural and dynamical consequences of this targeted attack to our spatial networks.

Since we wanted to study the capacity of the network to show global activity, we analyzed the evolution of both structural and functional global efficiencies as we increased the percentage of nodes deleted. The results are depicted in Fig. 10.

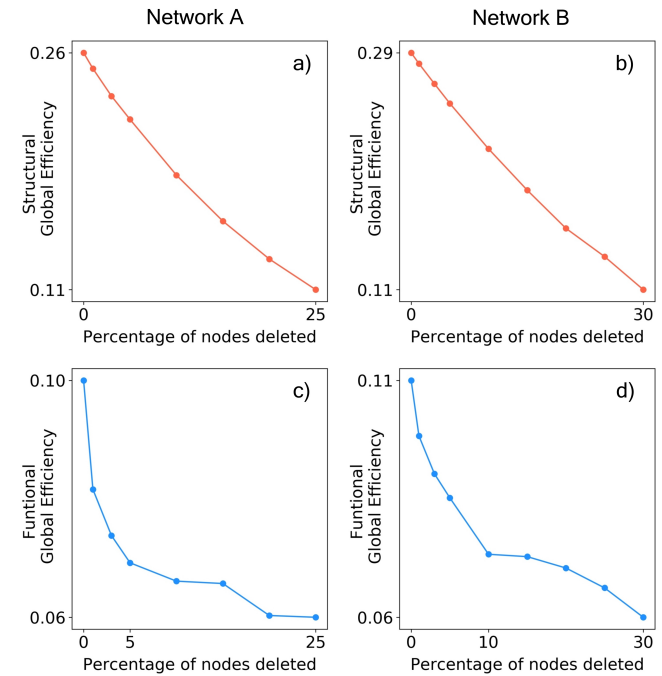


FIG. 10: Directed attack on Betweenness Centrality and its impact in global efficiency. (Left) Magnitudes computed for network A. (Right) Magnitudes computed for network B. (Top) Evolution of the structural global efficiency with respect to the percentage of nodes deleted. (Bottom) Evolution of the functional global efficiency with respect to the percentage of nodes deleted. The percentages explored have been 0, 1, 3, 5, 10, 15, 20 and 25 for network A and additionally 30 for network B.

Figures 10a and 10b show that, as the fraction of removed nodes increases, the structural global efficiency diminishes gradually, almost linearly. By contrast, Figs. 10c and 10d show that the functional global efficiency presents a substantial decrease for the first values of percentage followed by a less steep decline. The sharp drop of this magnitude for network A occurs for the first 3-5% of nodes removed. For network B it decreases sharply until the 10% of neurons have been deleted. These inflection points correspond to the moment where the network breaks apart in two, i.e., the two small modules are separated from the rest of the network.

If we analyse the raster plot of network A after removing 5% of the nodes, Fig. 11a, and of network B after removing the 10%, Fig 11b, we can identify the regions that belong to the two small modules (regions in orange) because in these regions neurons do not fire synchronously with the rest of the network.

The graphs of the two networks corresponding to these percentages of deleted highly central nodes are displayed

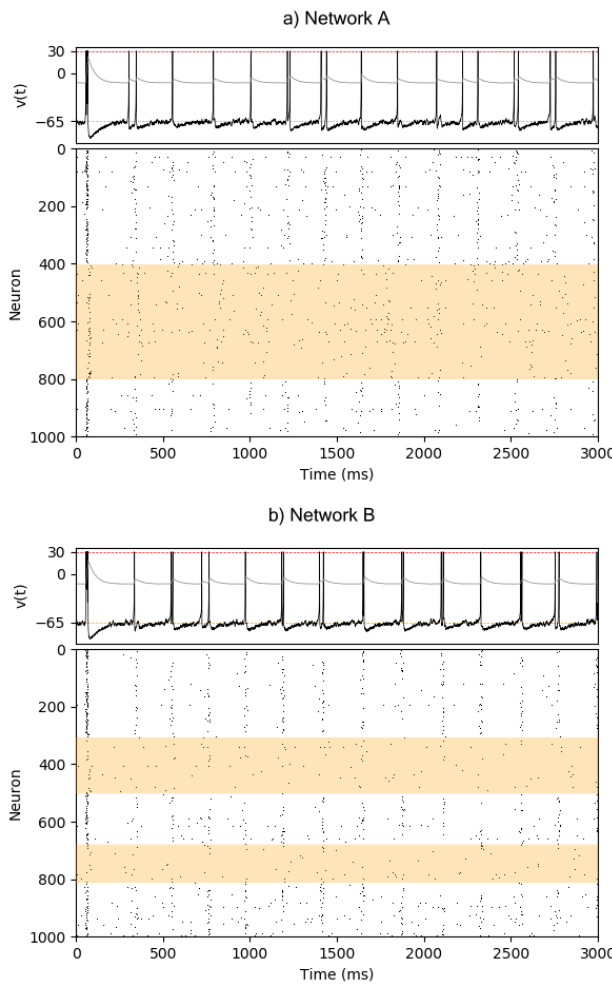


FIG. 11: Impact of targeted attack on collective dynamics. (Top) Network A with 5% damage on top–scoring structural betweenness centrality nodes. The upper panel shows the membrane potential of an excitatory neuron that participates in network bursts. The lower panel is the raster plot of the network. The region highlighted in orange corresponds to the modules that do not participate in collective activations, i.e. they are functionally affected due to damage. (Bottom) Equivalent analysis for network B with 10% node deletion.

in Fig. 12. Network A has two differentiated functional blocks almost independent from each other. In network B the splitting is not clear but a substantial decrease in the connections between the large module and the small one on the left can be observed.

By analysing the raster plots obtained from the simulations it can be seen that the large module keeps firing together. One needs to delete the 25% of nodes for network A and the 30% of nodes for network B for all traces of collective activity to disappear.

A possible explanation to the differences between the robustness of networks A and B is the difference in their structural betweenness centralities. Whereas network A has a few nodes with huge values of betweenness centralities that are therefore vital for the integration of the net-

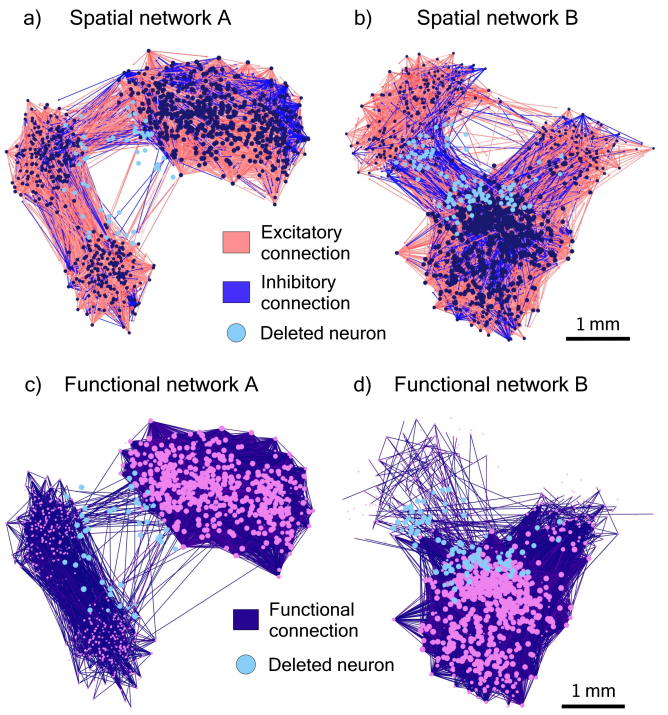


FIG. 12: Structural and functional network graphs for high damage. (Top) Structural graphs of the two networks, for 5% (network A) and 10% damage (network B), respectively. Excitatory connections represented in red and inhibitory connections in blue. Darker colors are related to stronger connections. Each black dot corresponds to a neuron. (Bottom) Corresponding graphs for the functional networks. All functional connections are represented in purple. Brighter tones are related to stronger connections. Each pink dot corresponds to a neuron. In all graphs the size of the dot is directly proportional to the number of connections of the neuron it represents and blue dots correspond to deleted neurons.

work, in network B the relative importance of its nodes is not so biased. Consequently, when the most central nodes of network A are attacked, more damage is being inflicted on the network.

VI. CONCLUSIONS

In silico modelling is a useful tool to investigate the relationship between the structural wiring of a network and the functional connections that emerge from it. In this project we have designed directed weighted networks with spatial constraints and we have simulated their dynamics through a slightly modified Izhikevich model.

Firstly, it has been proved that connectivity and synapse strength play a central role in the emergence of collective activity. In addition, a parametric analysis of the original Izhikevich model has been carried out to understand how its parameters influence the frequency of network bursts. It has been found that the frequency

of collective activity range from 4 to about 26 Hz, an observation that is consistent with the literature [21, 22].

Furthermore, we have compared the structural and functional connectivities of two networks (A and B), which at first glance seem quite similar, through the evaluation of their properties using the mathematical approach of graph theory. Not only has been found that the structural and functional connectivities of each network have quite different key properties, but also that although networks A and B have very similar functional connectivities, their structural networks are very different. Therefore, our study highlights the complexity and difficulty in obtaining the structural links of a network from the analysis of its functional connections.

Moreover, the results obtained for metric networks have been contrasted with null models. This has allowed us to pinpoint the importance of spatial embedding in the shaping of structural connections.

Finally, we have analyzed how the networks studied in this project behaved under damage. We have progressively removed some of their nodes in decreasing order of

betweenness centrality and we have found the percentage of nodes that have to be deleted so that the network bursts disappear.

Acknowledgments

I would like to thank my advisor Dr Jordi Soriano both for his invaluable help, endless patience, and encouragement during the development of this work and for passing on me his passion and enthusiasm for this fascinating field of research. I also thank Sergio Faci Lázaro for his help.

I am also indebted with the Institute of Complex Systems of the University of Barcelona (UBICS) for having awarded me with a collaboration fellowships to develop the Final Master's Thesis with one of their members.

Finally, I also want to express my gratitude to my parents and close friends for their constant unconditional support especially during the hardest moments of this year.

-
- [1] D. S. Bassett, O. Sporns, ‘Network neuroscience’, *Nat. Neurosci.* **20** (2017): 353
 - [2] J. Soriano, J. Casademunt, “Neuronal cultures: The brain’s complexity and non-equilibrium physics, all in a dish”, *Contrib. Sci.* **11**, 225-235 (2015)
 - [3] C.J. Honey, J.-P. Thivierge and O. Sporns, “Can structure predict function in the human brain?” *Neuroimage* **52**, 766–776 (2010)
 - [4] J. G. Orlandi, J. Soriano, E. Álvarez-Lacalle, S. Teller, J. Casademunt, “Noise focusing and the emergence of coherent activity in neuronal cultures”, *Nat. Phys.* **9** (9), 582-590 (2013)
 - [5] A.A. Ludl, J. Soriano, “Impact of Physical Obstacles on the Structural and Effective Connectivity of in silico Neuronal Circuits.” *Front. Comput. Neurosci.* **14**, 77 (2020)
 - [6] E. Tibau, A. Ludl, S. Rüdiger, J.G. Orlandi and J. Soriano, “Neuronal Spatial Arrangement Shapes Effective Connectivity Traits of in vitro Cortical Networks” *IEEE Trans. Netw. Sci. Eng.* **7** (1), 435-448 (2020)
 - [7] E. Bullmore, O. Sporns “Complex brain networks: graph theoretical analysis of structural and functional systems.”, *Nat. Rev. Neurosci.* **10**, 186–198 (2009)
 - [8] S. Boccaletti, et al., “Complex networks: Structure and dynamics.”, *Phys. Rep.* **424** (4-5), 175-308 (2006)
 - [9] C.J. Stam et al. “Graph theoretical analysis of magnetoencephalographic functional connectivity in Alzheimer’s disease.” *Brain* **132**, 213-224 (2009)
 - [10] S. Faci-Lázaro, J. Soriano, J. Gómez-Gardeñes, “Impact of targetted attack on the spontaneous activity in spatial and biologically-inspired neuronal networks”, *Chaos* **29**, 083126 (2019)
 - [11] V. Braintenberg, A. Schüsz “Statistics and Geometry of Neuronal Connectivity”, Springer, Berlin, (1998)
 - [12] E. M. Izhikevich, “Simple model of spiking neurons”, *IEEE Trans. Neural Netw. Learn. Syst.* **14**, 1569-1572 (2003)
 - [13] H. Dale, “Pharmacology and Nerve-endings”. *Proc. R. Soc. Med.* **28** (3): 319-332, (1935)
 - [14] J. Soriano, J. Casademunt ”Neuronal cultures: The brain’s complexity and non-equilibrium physics, all in a dish”, *Contrib. Sci.* **11**, 225-235 (2015)
 - [15] Neuroanatomy, Neuron Action Potential <https://www.ncbi.nlm.nih.gov/books/NBK546639/>
 - [16] KenHub: Action potentials <https://www.kenhub.com/en/library/anatomy/action-potential>
 - [17] A.L. Hodgkin, A.F. Huxley ”A quantitative description of membrane current and its application to conduction and excitation in nerve”, *J. Physiol.* **117**, 500-544, (1952)
 - [18] L. Hernández-Navarro et al. “Noise-driven amplification mechanisms governing the emergence of coherent extreme events in excitable systems.”, *Phys. Rev. Research* **3**, 023133 (2021)
 - [19] V.D. Blondel et al., “Fast unfolding of communities in large networks”, *J. Stat. Mech.* **10**: 10008 (2008)
 - [20] H. Yamamoto et al., “Impact of modular organization on dynamical richness in cortical networks”, *Sci. Adv.* **4**, eaau4914 (2018)
 - [21] G.E. Soares et al., “ Emergence of synchronicity in a self-organizing spiking neuron network: an approach via genetic algorithms”, *Nat. Comput.* **11**, 405–413, (2012)
 - [22] L.D.R. Oliveira et al., “Effects of the parameters on the oscillation frequency of Izhikevich spiking neural networks”, *Neurocomputing* **337**, 251-261, (2019)
 - [23] P. Erdos and A. Rényi, “On Random Graphs”, *Publicationes Mathematicae (Debrecen)* **6**, 290-297 (1959)
 - [24] R.L. Buckner et al., “Cortical Hubs Revealed by Intrinsic Functional Connectivity: Mapping, Assessment of Stability, and Relation to Alzheimer’s Disease”, *J. Neurosci.* **29**(6), 1860-1873, (2009)
 - [25] Y. He, Z. Chen and A.C. Evans, “Structural insights into aberrant topological patterns of large-scale cortical networks in Alzheimer’s disease.” *J. Neurosci.* **28**, 8148–8159, (2008)